International Journal of Applied Pharmaceutics

ISSN- 0975-7058 Vol 14, Issue 2, 2022

Original Article

FORMULATION AND EVALUATION OF TWO CELASTROL NANOEMULSIONS PREPARED FROM TWO OILS: ISOPROPYL MYRISTATE AND VIRGIN COCONUT OIL

NUR ALAM ABDULLAH[1], MAHDI JUFRI[2*], ABDUL MUN'IM[3], FADLINA CHANY SAPUTRI[4]

[1]Student of Pharmaceutical Sciences, Faculty of Pharmacy, University of Indonesia, [2]Department of Pharmaceutical Technology and Drug Development, Faculty of Pharmacy, University of Indonesia, [3]Department of Pharmacognosy and Phytochemistry, Faculty of Pharmacy, University of Indonesia, [4]Departemen Pharmacology and Pharmacokinetics, University of Indonesia, Depok, 16424, University of Indonesia
[*]Email: mahdi.jufri@farmasi.ui.ac.id

Received: 03 Nov 2021, Revised and Accepted: 18 Dec 2021

ABSTRACT

Objective: Celastrol, which is classified as BCS 4, needs to be developed into a nanoemulsion formula for a stable and good formulation. The aim of the study was to determine the *in vitro* penetration ability and adsorption efficiency (EE) between two different base oils, namely Isopropyl myristate (IPM) and virgin coconut. oil (VCO).

Methods: Two celastrol nanoemulsion formulas were prepared by high energy method using High share homogenizer (HSH) at 15,000 rpm for 15 min, using different oil-based components, F1 IPM and F2 VCO. Particle size, polydispersity index (PDI), D90, zeta potential, and morphology of nanoemulsions was evaluated. *In vitro* studies by Franz diffusion cell test method determined the difference.

Results: The results showed that celastrol can be formulated well with a ternary ratio of 5:45:50 for IPM and 20:30:50 for VCO. The absorption efficiency test for celestrol levels was 96.49%±2.72 for IPM and 76.53%±1.19 for VCO. The mean particle size, PDI, and zeta potential were 70.81±0.20 nm, 0.1±0.03, and 50.2±0.60 mV, for VCO and 186.23±3, respectively. 12 nm, 0.2±0.07, and 45.5±1.10 mV for HDI. Spherical morphology<200 nm. Franz diffusion *in vitro* at 20 and 24 h, celastrol is well penetrated at levels of 2.4 g/ml gram and 2.5 g/ml for HDI and at 2.0 g/ml gram and 2.4 g/ml, respectively. ml/gram for VCO.

Conclusion: Celastrol was successfully developed into nanoemulsions using IPM or VCO, particle size<200 nm, and stable spherical shape.

Keywords: Celastrol, Nanoemulsion, VCO, IPM, Particle size

DOI: https://dx.doi.org/10.22159/ijap.2022v14i2.43509. Journal homepage: https://innovareacademics.in/journals/index.php/ijap

INTRODUCTION

Celastrol (2*R*,4a*S*,6a*S*,12b*R*,14a*S*,14b*R*)-10-Hydroxy-2,4a,6a,9,12b,14a-hexamethyl-11-oxo-1,2,3,4,4a,5,6,6a,11,12b,13,14,14a,14b-tetradeca-hydropicene-2-carboxylic acid), is a nutritious compound derived from *Tripterygium wilfordii* Hook F isolates [1]. Celastrol can be used to treat several immune system disorders and is neuroprotective. The compound can be used as an anti-inflammatory for various causes of inflammation, especially autoimmune disorders. Celastrol has a Log P value of 5.63 and is a Biopharmaceutical Classification System (BCS) IV (low solubility, low permeability) compound [2].

To overcome this problem, celastrol can be developed by using a nanotechnology approach, which aims to increase this biological compound's solubility and permeability, One type of nanotechnology is a nanoemulsion preparation. Nanoemulsions have particle sizes between 100 and 500 nm [3, 4].

Previous research using a nanoemulsion preparation of celastrol isopropyl myristate (IPM) to form the oil phase showed that it was stable for the 3-month test period. In our current research, we have used virgin coconut oil (VCO) to form the oil phase. VCO is a natural oil originating from Indonesia [5, 6].

There are currently three methods of making nanoemulsion formulations, titration, low energy, and high energy. Nanoemulsions tend to be opaque (cloudy), whereas microemulsions tend to be transparent. These types of preparations and their various formulations can be distinguished by their particle size, structural shape, and degree of stability [7]. This study aimed to compare celastrol nanoemulsions prepared from two different oils: IPM and VCO.

MATERIALS AND METHODS

Materials

Standard celastrol was ordered from Sigma Aldrich. Celastrol samples were also obtained from Xi'an Fengzu Biological Technology Co., Ltd. (China). Isoprophyl myristate (IPM) was purchased from Merck, and virgin coconut oil (VCO) purchased from CV. Vicoma (Samani Island Cilacap-Central Java. Polysorbate 80 (Tween 80), propyleneglycol (PG), methylparaben, prophyl paraben,, ethanol 70%, triethanolamine, Sepigel® 305 from PT. Brataco, Tbk. and aqua pro injections, were purchased from Acetonitrile pro analysis, concentrated formic acid, and methanol pro analysis were purchased from Merck.

Equipment

Glass beakers, measuring cups (Pyrex®), high-shear homogenizer (HSH) (Ultra Turrax 1000 x T25 Digital disperser; IKA Works Inc., Wilmington, NC, USA), thermometer, sonicators, high-performance liquid chromatograph (HPLC) (Shimadzu, Japan), digital scales, Viscometers (Brookfield and Cole Parmer), pH meter, particle size analyzer (Malvern®), and electric oven.

Method

The nanoemulsion bases prepared by using an Ultra Turrax disperser HSH device at a speed of 25,000 rpm for 20 min followed by sonication. Starting with the preformulation, we measured the nanoemulsion areas and developed a ternary diagram by using the Chemix 7.00 series program [8].

Chromatography conditions and instruments

Preliminary testing involved identifying the purity of the celastrol standard and celastrol samples. By performing HPLC on a Shimadzu® LC 20 AT HPLC instrument using a Sunfire™ C18 column (5 µm, 4. 6 x 250 mm), and a ultraviolet absorbance detector. at a wavelength of 230 nm.

The HPLC mobile phase was HPLC-grade acetonitrile: 0.1% formic acid in water at 85:15, injection volume of 20 µl, and flow rate of 1 ml/minute. The celastrol concentrations for the calibration curve

ranged from 0.031 ppm (lowest concentration of the dose to be developed into a nanoemulsion to 2.5 ppm.

Construction of a pseudo-ternary phase diagram

The nanoemulsion base was made by compiling the ratios of the VCO and Smix oil phases. The Smix was a combination of surfactants and cosurfactants (Tween 80 and PG) from the smallest to the largest proportions (1: 9 to 9:1), whereas the water phase was slowly titrated while stirring using the HSH tool at high speed. (30,000 rpm for 20 min). The results of the nanoemulsion preparations that were made were observed and arranged into a ternary phase diagram by using the Chemix 7.00 series program [9, 10].

Table 1: Oil phase ratio and smix

Ratio smix	Smix	Oil phase	Water phase
1: 9	45	5	X
2: 8	40	10	X
3: 7	35	15	X
4: 6	30	20	X
5: 5	25	25	X
6: 4	20	30	X
7: 3	15	35	X
8: 2	10	40	X
9: 1	5	45	X

*X: Amount of water sought

Selection of the nanoemulsion base formulation

After all of the basic formulas were made, particle size analysis was performed on a Malvern® particle size analyzer. The particle size results for all nanoemulsion base preparations were compared and arranged into the Chemix 7.00 series program to determine which formulas met the criteria for nanoemulsion preparations. The nanoemulsion areas were plotted on the ternary diagram.

Preparation of nanoemulsions with celastrol

After determining the nanoemulsion base formulation that met the criteria of a particle size<200 nm at D90, we added the active pharmaceutical ingredient to the selected nanoemulsion base formulation.

A 10.0 mg amount of celastrol was accurately weighed and placed in a 10.0-ml Erlenmeyer flask, and then methanol was added to the volume. A 500-µl aliquot was then pipetted into a glass beaker that contained all of the formulation ingredients. In the selected proportions. The formulation was homogeneated by using an Ultra Turrax disperser at 15,000 rpm for 15 min.

Evaluation and characterization of base preparations

Organoleptic examination, pH

The preparations were then subjected to physical and visual examinations to evaluate their form, color, odor, and pH.

Viscosity of preparations

The thickness of the nanoemulsion preparation was measured by using a viscometer (Cole Parmer).

Entrapment efficiency (EE)

To test the recovery of celastrol from each of the nanoemulsions formed, namely VCO and IPM, then in each tested formulation, we accurately weighed 1 gram of the prepared nanoemulsion into a centrifuge tube and then added 5 ml of methanol. The mixture was filtered through a syringe filter and then analyzed by HPLC at a wavelength of 230 nanometers (nm), a flow rate of 1 ml, and an injection volume of 20 l, with a mixture of acetonitrile mobile phase and 0.1% formic acid solution at a ratio of 85:15 on a Zorbax column. C18 XDB The celastrol content of the two preparations was calculated using the formula in the fig. 2.

$$\text{Entrapment Efficiency (\%)} = \frac{\text{AA concentration measured}}{\text{AA concentration in teoritical}} \times 100$$

Nanoemulsion base formula morphology

In the morphological test stage, transmission electron microscopy (TEM) was performed by dropping 0.2 µl of the nanoemulsion sample onto a grid plate and adding 2% uranyl acetate dye, then observing it under the TEM microscope.

Cycling test

The resistance cycle of the preparation over a time period and temperature range that varied from 4 °C, 28 °C, and 40 °C for approximately 12 consecutive days. At each organoleptic examination, the pH and concentrations of the celastrol active substances were measured. The base formula was selected according to the nanoemulsion criteria.

From this screening stage, we selected the nanoemulsion preparation that contained the highest standard celastrol concentration.

***In vitro* franz diffusion cells**

The penetration ability of celastrol into the skin membrane above the stomachs of Sprague–Dawley white rats weighing 200 to 250 g was measured. The Franz diffusion cell test method was used on a membrane area of 1.76 cm^2. First, the mouse's hair was cut with an electric shaver, then the selected part of the skin over the stomach was removed and stored in a freezer at 21 °C for 24 h for next-day use. The next day, a penetration test was performed by placing the skin on the Franz diffusion cell test kit in which the upper part of the donor is the stratum corneum and the lower part is the acceptor of the cell recipient. Inside the device was a liquid phosphate buffer solution at a pH of 7.4. The solution was stirred at 100 rpm at 37 °C±0.5 °C. A 1-gram amount of celastrol nanoemulsion was weighed and inserted into each donor compartment successively at time intervals of 0, 2, 4, 6, 8, 10, 12, 20, and 24 h.

The sink condition must be considered in every step-by-step test sampling. Approximately 1 ml of each sample was taken for HPLC analysis at a wavelength of 230 nm. All *in vitro* procedures received ethical approval to obtain male Sprague Dawley (SD) rat skin obtained from Bogor Agricultural University (IPB), with ethical approval from the Faculty of Medicine, the University of Indonesia (No.: KET-1067/UN2. F1/ETIK)./PPM.00.02/2019), at following the research guidelines including all rats undergoing a standard acclimatization process for 2 w before being given treatment including adequate feeding and drinking.

RESULTS AND DISCUSSION

Basis for selecting nanoemulsion constituent materials

The materials in the nanoemulsion preparation were selected to have lipophilicities similar to those of the active celastrol. An example is the selection of Tween 80 as the surfactant because of its medium-chain triglyceride (MCT) group and its fairly stable characteristics, making it a good component in the base for the colloid preparations. Similarly, propyleneglycol was chosen as a co-surfactant to help accelerate the formation of spherical nanoemulsion droplets [11].

Chromatography conditions and instruments

Celastrol was detected at a wavelength of 230 nm at 3.4 min in the HPLC purity analysis of the celastrol standard and samples can be seen in fig. 1 and 2. The analysis used a mobile phase mixture of

acetonitrile and 0.1% formic acid solution at a ratio of 85:15 and a C18 column, the flow rate of 1.0 ml, and an injection volume of 20 µl. The analysis was performed at six celastrol concentrations to determine the linearity of the calibration curve.

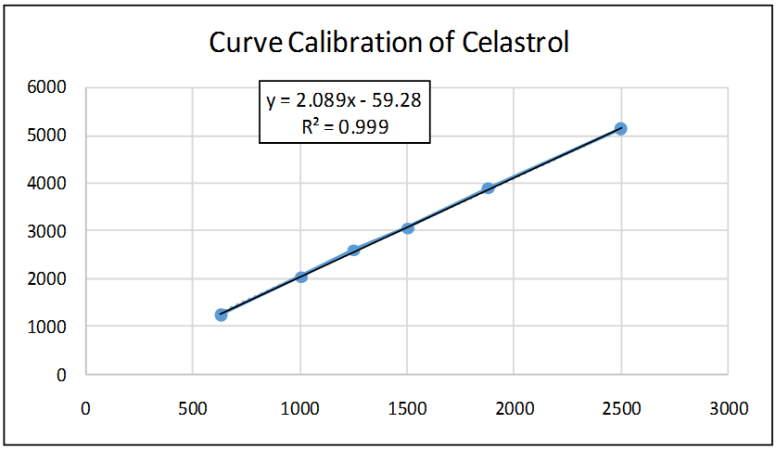

Fig. 1: Celastrol peak in the HPLC calibration curve

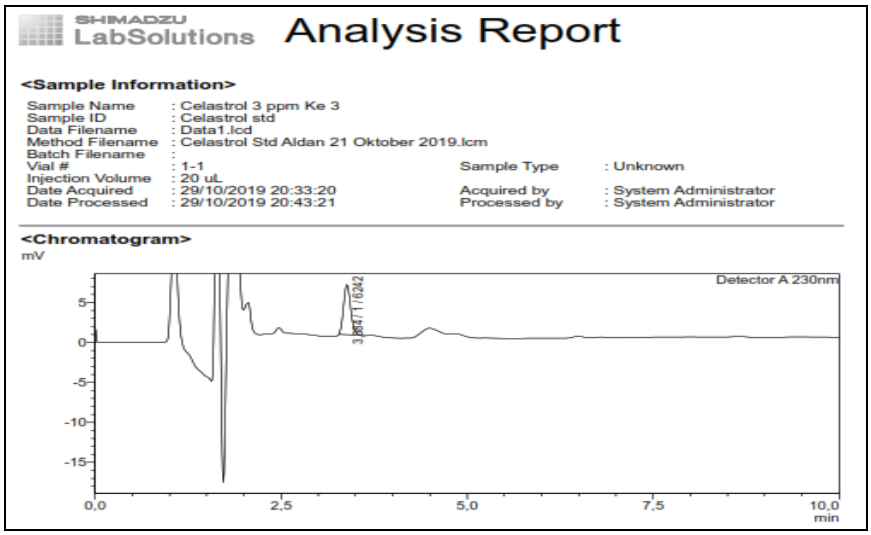

Fig. 2: Celastrol chromatogram in the HPLC

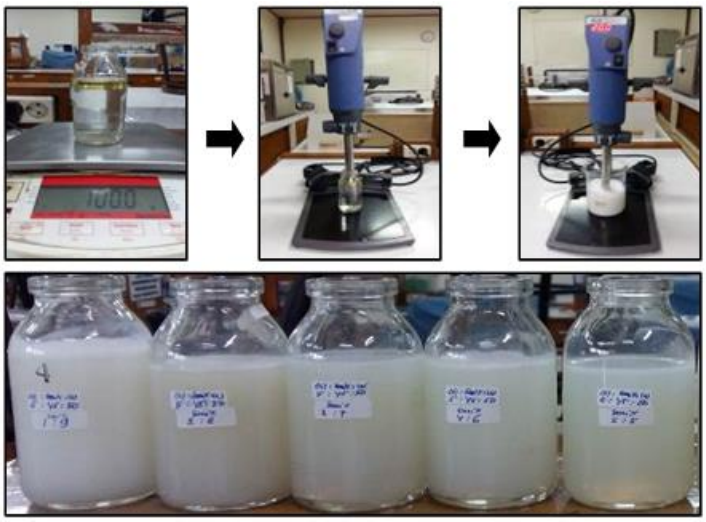

Fig. 3: Pre formulation of the base nanoemulsion after high-shear homogenization

Nanoemulsion base preparation and characterization

The nanoemulsion base preformulation can be seen in fig. 3. process was carried out without adding celastrol, with the aim of evaluating the extent to which the nanoemulsion base formed with properties close to the target nanoemulsion properties, which were an average particle size<200 nanometers (nm), polydispersity index (PDI) from 0.1 to 0.3, and a zeta potential range from −30 to+30 mV [12, 13].

Before obtaining the ideal nanoemulsion base, several steps were carried out during the preformulation to determine which formulation was best for delivering celastrol A series of numbers were compiled from the components of the nanoemulsion base into a comparison table to obtain an arrangement based on 1 to 9 parts and 9 to 1 parts of each constituent component, including IPM or VCO as the oil phase in this case, with the Tween 80 surfactant and propylene glycol and distilled water as the water phase. These comparison values were placed into the ternary system in the form of an isosceles triangle diagram so that the characteristics of each nanoemulsion base preformulation could be more easily evaluated [14, 15].

The developed pseudo-ternary system shows the particle sizes of the preformulations in relation to the nanoemulsion preparation particle size requirements, ranging from 100 an 500 nm) [16]. Twelve nanoemulsion base preformulas, six each for IPM and VCO, were evaluated. The 12 pre formulations were evaluated by measuring the particle sizes on the Malvern particle size analyzer After the measurements were performed, the next step was to compile all of the preformulations into a pseudo-ternary diagram to determine which formulas could form a nanoemulsion area based on the particle size obtained (fig. 5) The mean particle size D90 of the nanoemulsion base preformulation was 343 nm for IPM and 380 nm, for VCO, which met the basic requirements of the desired nanoemulsion base [17].

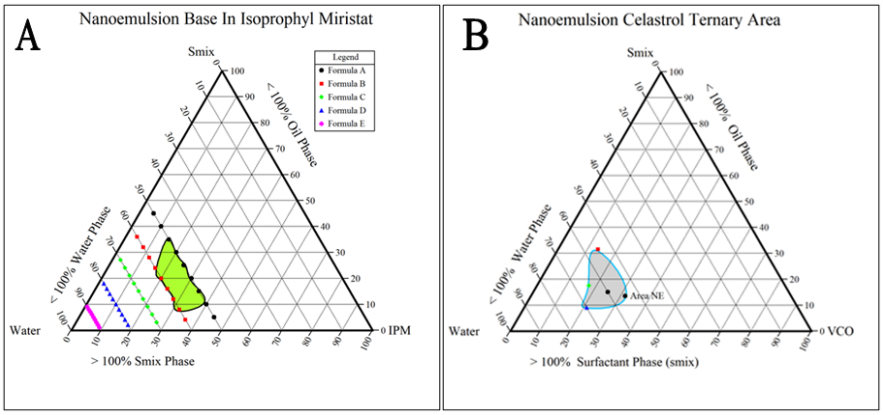

Fig. 4: Pseudo-ternary diagram of the nanoemulsion based preformulations using A. IPM and B. VCO oil phases

The pseudo-ternary diagram of the two oil phases shows the different nanoemulsion areas formed in the preformulation base can be seen fig. 4. For IPM, it can be seen that the areas that form a nanoemulsion are in the oil ratio range of 5:45:50, whereas for VCO, the areas that form a nanoemulsion are in the oil ratio range of 20:30:50. This data shows the differences and similarities of the properties of the two oil phases of the nanoemulsion preparation but that both form a stable, ideal nanoemulsion base. This could also be because the IPM and VCO are from different sources [18]. IPM has a synthetic MCT oil group, which tends to be more often used in cosmetics. VCO is sourced from vegetable oil and is prone to oxidation and reduction reactions which can affect the shelf life of pharmaceutical preparations with VCO, so it is still necessary to modify the formulation to produce a nanoemulsion base that is resistant to environmental changes that might affect the stability [19].

Table 2: Particle size results for the selected preformulations

No	Surfactant with Co-surfactant	Oil (VCO) →Smix ratio 30	Oil (IPM)	20 (VCO) 45	SD (±)	5 (IPM)	SD (±)
1	Z-Average (nm)	1	1	134.3	45,12	155.8	21,34
	PDI			0.3	0,14	0.72	0,06
	D90 (nm)	9	9	380	1040,20	276.4	40,10
	Zeta (mV)			−4.16	5,53	−41.3	0,24
2	Z-Average (nm)	2	2	113.3	12,91	151	16,77
	PDI			0.4	0,07	0.23	0,06
	D90 (nm)	8	8	335	633,10	208.4	15,57
	Zeta (mV)			−4.6	2,15	−34.6	2,29
3	Z-Average (nm)	3	3	70.81	0,20	186.23	3,12
	PDI			0.1	0,03	0.2	0,07
	D90 (nm)	7	7	120	3,46	117	1,00
	Zeta (mV)			−50.2	0,60	−45.5	1,10
4	Z-Average (nm)	4	4	115.3	47,94	230.1	15,36
	PDI			0.3	0,26	0.39	0,06
	D90 (nm)	6	6	354	2459,03	465.3	57,55
	Zeta (mV)			−4.33	6,08	−37.1	2,29
5	Z-Average (nm)	5	5	106.2	2,62	182.2	76,56
	PDI			0.3	0,21	0.27	0,15
	D90 (nm)	5	5	323	1591,74	200.2	68,82
	Zeta (mV)			−6.55	2,89	−28.3	66,33
6	Z-Average (nm)	6	6	138.7	179,23	169.7	73,84
	PDI			0.2	0,06	0.25	0,17
	D90 (nm)	4	4	336	585,61	216.8	432,81
	Zeta (mV)			−4.2	8,14	−25.4	4,03

Repetition three times analysis data, value is mean±SD (n = 3)

After the celastrol nanoemulsion formulation was selected on the basis of the preformulation, the characteristics of the celastrol nanoemulsion preparations with each of the two oils were analyzed. The results of these tests are presented in table 2 and fig. 5. It can be seen that for the celastrol nanoemulsion with the VCO oil phase, the average particle size is 70.81±0,20 nm, D90 of 120±3,46 nm, with a PDI of 0.1±0,03 and a zeta potential of −50.2±0,60 mV. For the celastrol nanoemulsion using IPM as the oil phase, the average particle size was 186.23±3, 12 nm, with a D90 of 117±1,0, PDI of 0.2±0,07, and a zeta potential of −45.5±1,10 mV. The other formulations showed varying particle sizes with some prerequisite characteristics for nanoemulsion preparations that did not meet the appropriate criteria, so those formulations were not selected [20, 21].

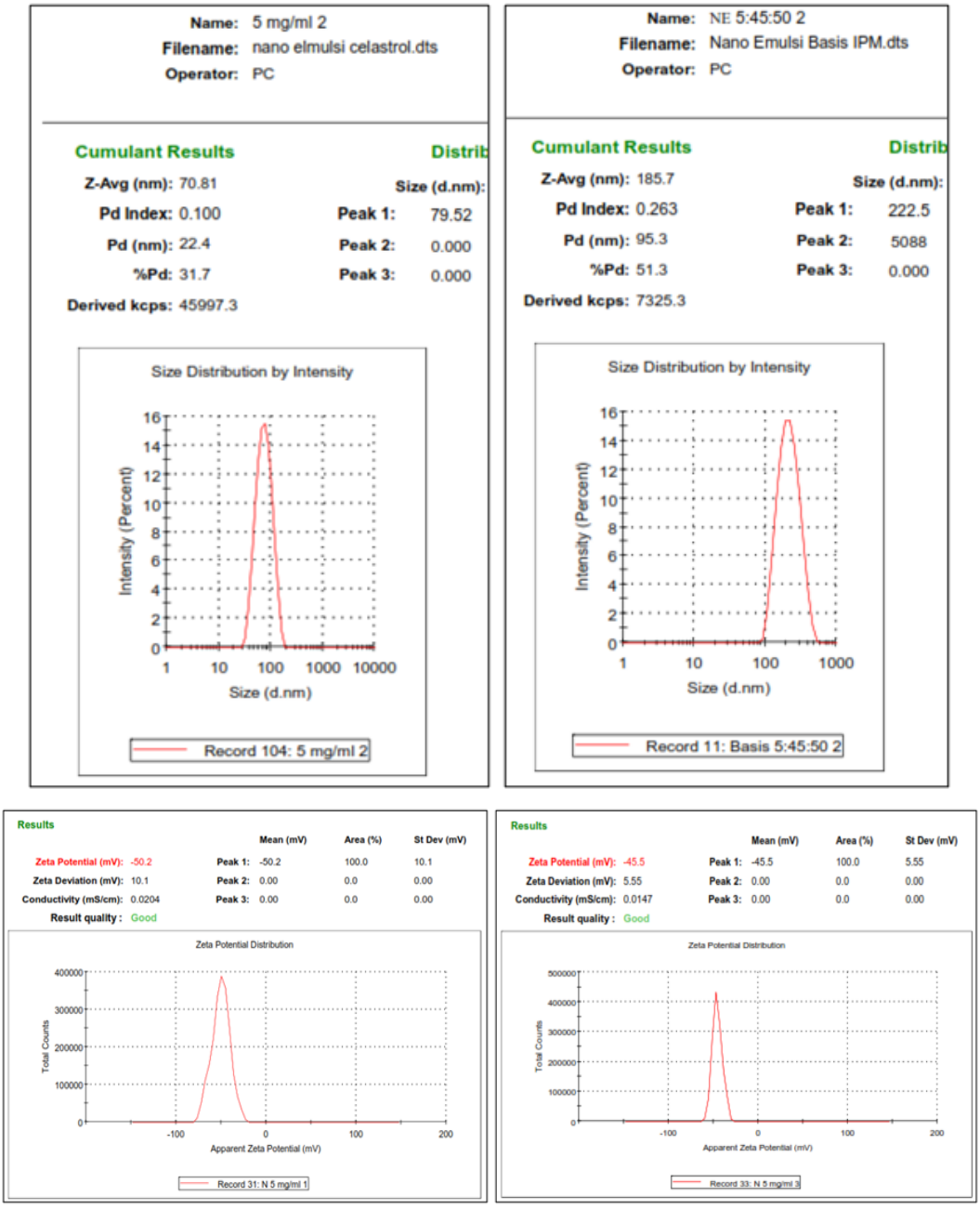

Fig. 5: Particle sizes and zeta potentials of the formulations with IPM and VCO as the oil phases

Organoleptic examination, pH

For the examination of nanoemulsion preparations from the two oil phases, the physical appearance of the two preparations did not show a striking difference in the white and slightly yellow color due to the celastrol compound as the active pharmaceutical ingredient. The odor did not show a rancid odor for 12 experimental cycles, and the preparation was not sticky to the touch. However, the first pH measurements were 7.6 for the nanoemulsions using IPM and 6.8 using VCO. Furthermore, the pH values of the two preparations were different, and both tended to decrease in the pH range of 4.5 6.0 over the 12-day daily testing can be seen fig. 6.

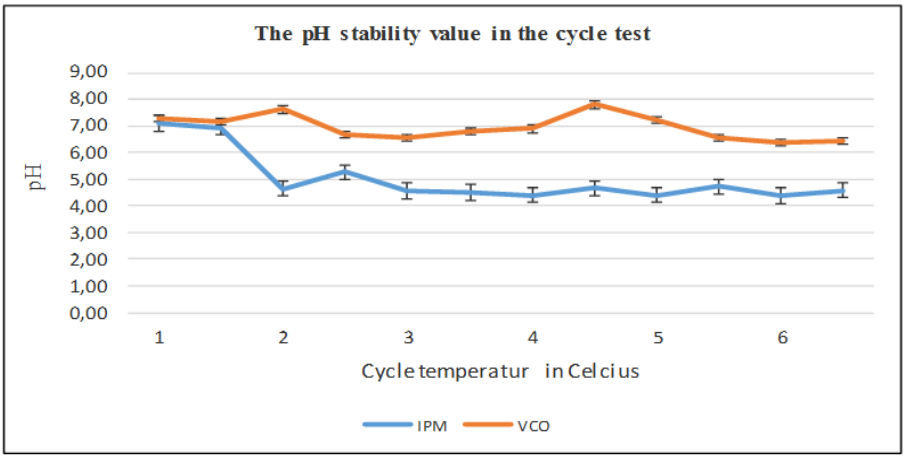

Fig. 6: Variations in pH over 12 d, Repetition three times analysis data, value is mean±SD 1,40 (n = 3)

This pH behavior reportedly occurs because the components of the two preparations were presented in a fresh state even though pure celastrol had its own significant acidity, but when mixed with other ingredients, there was an increase in the pH value closer to neutral. However, the pH values of the two preparations tended to decrease has become commonplace due to variations in temperature Mook *et al.* found that when the oil phase in a colloid dosage form was mixed with the water phase, CO_2 gas would eventually form after storage at high temperatures [22].

Viscosity of preparations

The viscosity of a pharmaceutical preparation is an indicator of the product's long-term (years) stability under storage conditions. Therefore, the viscosity of colloid-based preparations must be determined to see if preparations remain stable in their physical form when in production or change from semi-solid to less viscous or even to a liquid during storage different temperature conditions [23].

From the measurement results, the viscosity value for the nanoemulsion preparations with IPM was 20 cP and with VCO was 27.9 cP using spindles 4 and 5, which showed thixotropic plastic flow for IPM and anti-thixotropic plastic for VCO. Fig. 7 shows that the two preparations similar at the beginning of the measurement due to the shear rate of the measuring device not starting from the zero point where the shear stress works by cutting the Y-axis. The IPM preparation showed anti-thixotropic plasticity because the instantaneous energy when the preparation is shaken increases the viscosity, which soon returns to its original form. Furthermore, for VCO, it can be seen in the graph that the shape of the flow is thixotropic plastic; when the nanoemulsion preparation is shaken it will change to a dilute form, but only for a moment—when it is left idle, the preparation will return to its original state [24].

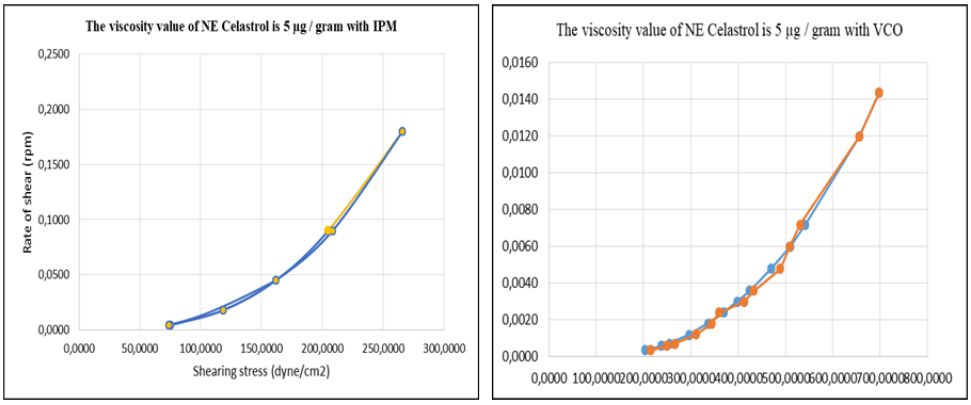

Fig. 7: Graph of viscosity IPM and VCO in nanoemulsion

Based on the results obtained from the two oil phases, the IPM, which is sourced from synthetic oil, shows relatively longer stability than the stability of the nanoemulsion preparations containing VCO. At a temperature of 40 ° C at week 7, a liquid was found in the preparation, which indicated that celastrol NEG from VCO experienced syneresis. This is supported by the zeta potential of −10.1 mV for VCO and −22.5 mV for IPM, which are intended as parameters indicative of the long-term stability during storage at various temperatures and in different environments. This finding indicates that every positive-or negative-charge shift in the globule system of the colloid particle component shows rapid aggregation. If the zeta potential test results of a nanoemulsion are close to zero (0), the stability of the particles tends to be short for storage and transportation of>3 mo for pharmaceutical preparations [25].

The IPM structure in fig. 8, does not contain medium and long chains, whereas VCO tends to have medium chains up to C12, which are physically and chemically disturbed by oxidation reactions due to the influence of temperature and heat during the storage process. Hydrolysis will accelerate the rancidity of VCO oil [26].

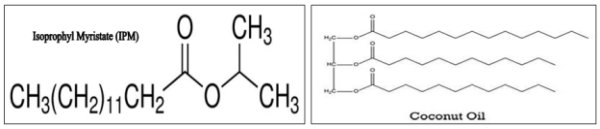

Fig. 8: Structures of IPM and VCO

Entrapment efficiency (EE)

The absorption efficiency of celastrol in the nanoemulsion preparations was tested by the direct method. The recovery test for the celastrol compound from the two nanoemulsion dosage forms gave IPM levels of 96.49% for IPM and 76.53% for VCO (fig. 9) [27].

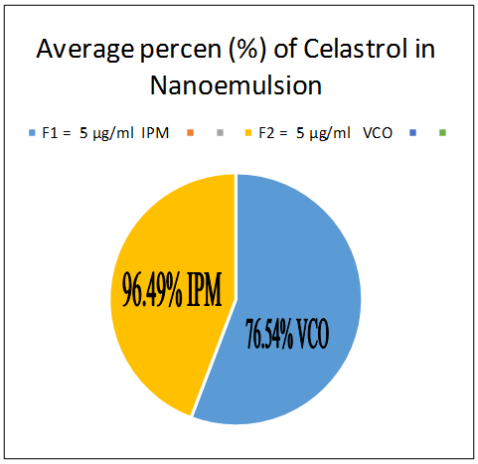

Fig. 9: Entrapment efficiency of celastrol in nanoemulsions with IPM and VCO, repetition three times analysis data, means (SD) F1±2,72 (IPM), F2±1,19 (VCO)

Nanoemulsion base formula morphology

In every development of colloid-based dosage formulations, especially nanoemulsions, morphological characterization of the droplets, including particle size, must be performed. High magnification is needed so that the particles can be seen clearly to determine if they are in accordance with the research objectives and match the results of previous particle size examinations.

The nanoemulsion preparation being developed is required to have the ideal morphological structure, including an intact or spherical shape of the nanodroplet. This is intended to support and ensure that the nanoemulsion preparation developed meets the size requirements in the range of 10–500 nm and match the existing particle size results. Producing a good morphological nanoemulsion form is very helpful. The preparation must be properly absorbed or penetrated into the body depending on the route the preparation is intended for. Therefore, characterization of nanoemulsion preparation formulations helps in selecting and sorting the constituent components of the nanoemulsion formulations Morphology can greatly affect the stability and continuity, and the shape of the particles in preparation is closely related to particle size and other parameters [28].

In this study, we found that the shape of the morphological of the two IPM and VCO nanoemulsion preparations were quite different visually, as shown in fig. 10. For the IPM, preparation, the nanodroplets depicted are slightly spherical and not uniform in overall particle size. This finding is thought to be due to a change in the physical structure of the components of the IPM and VCO nanoemulsion preparations, for which the oils have different sources in addition to their chemical properties, which can be influenced by pressure and temperature changes during nanoemulsion manufacturing [29, 30].

The shape of the IPM nanoemulsion droplets does not appear to be completely uniform in particle size, but it is sufficient to see the nanodroplet shape, which is close to spherical. This non-uniformity can be caused by the energy imparted during the manufacturing process. In this case, we suspected that the manufacturing had not followed the process rules, specifically, the first 5 min of homogenizing the mixture, the second 5 min in which large globules are reduced to small droplet globules, and the last 5 min in which the particle size of the previous droplets is reduced [31]. This method is considered to be very effective and efficient in obtaining nanoemulsion nanodroplets of the desired size. However, the droplet morphology of the nanoemulsion with VCO appeared to be good enough to form spherical droplet sizes. This finding proves that the method for making formulations has appropriate procedures and is capable of producing sizes and shapes that meet the requirements of the preparation [32, 33].

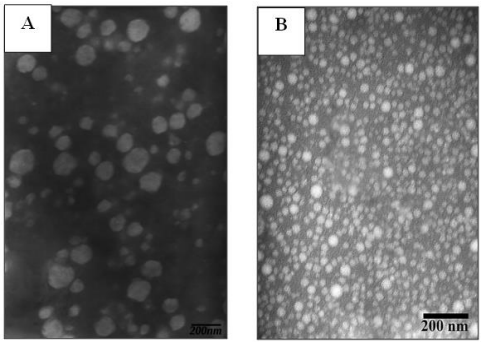

Fig. 10: TEM images showing the morphologies of the two celastrol nanoemulsions (A) IPM and (B) VCO

***In vitro* release study**

The *in vitro* profiles of Franz diffusion cells showed moderately good penetration rates for the IPM and VCO nanoemulsions. The results of the analysis show that the IPM nanoemulsion was slightly superior to the VCO nanoemulsion (fig. 11). At 20 and 24 h, the penetrated celastrol levels were 2.4 µg/ml/gram and 2.5 µg/ml/gram, respectively, for IPM and 2.0 µg/ml/gram and 2.4 µg/ml/gram, respectively, for VCO. Both nanoemulsions show fairly good ability to penetrate is zero order, so it is hoped that the levels of the active pharmaceutical ingredients will also be higher and maintained according to the desired therapeutic level. Thus, the nanoemulsion formulation for the delivery of celastrol is recommended for further research.

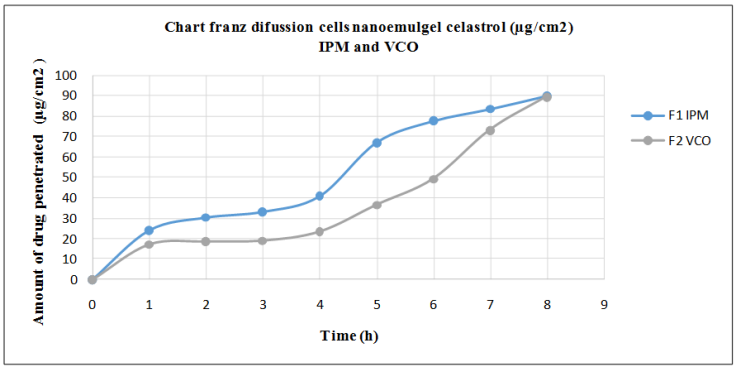

Fig. 11: *In vitro* profiles of Franz diffusion cells for the IPM and VCO nanoemulsions with celastrol, values are mean±SD, n=3, P 0,0064<0.05

CONCLUSION

This study shows that celastrol can be developed into colloidal preparations in nanoemulsions made from two oils: IPM and VCO, with an average droplet size of<200 nm by using Ultra Turrax HSH high energy homogenization without having to use a homogenizer High pressure (HPH).

ACKNOWLEDGMENT

The authors gratefully acknowledge the Directorate of Research and Community Engagements of Universitas Indonesia for financial support: Hibah PUTTI TADOK NKB-3190/UN2. RST/HKP.05.00/ 2020.

AUTHORS CONTRIBUTIONS

Nur Alam Abdullah was the main researcher and conducted research throughout the entire project and wrote the manuscript under the guidance of Mahdi Jufri, Abdul Mun'im, and Fadlina Chany Saputri.

CONFLICT OF INTERESTS

The authors declare that they have no conflicts of interest.

REFERENCES

1. Peng X, Wang J, Song H, Cui D, Li L, Li J, Lin L, Zhou J, Liu Y. Optimized preparation of celastrol-loaded polymeric nanomicelles using rotatable central composite design and response surface methodology. J Biomed Nanotechnol. 2012;8(3):491-9. doi: 10.1166/jbn.2012.1398, PMID 22764419.
2. Kang Q, Liu J, Zhao Y, Liu X, Liu XY, Wang YJ, Mo NL, Wu Q. Transdermal delivery system of nanostructured lipid carriers loaded with celastrol and indomethacin: optimization, characterization and efficacy evaluation for rheumatoid arthritis. Artif Cells Nanomed Biotechnol. 2018;46(Suppl3):S585-97. doi: 10.1080/21691401.2018.1503599, PMID 30306802.
3. Singh Y, Meher JG, Raval K, Khan FA, Chaurasia M, Jain NK, Chourasia MK. Nanoemulsion: concepts, development and applications in drug delivery. Journal of Controlled Release. 2017;252:28-49. doi: 10.1016/j.jconrel.2017.03.008.
4. Chime SA, Kenechukwu FC, Attama AA. Nanoemulsions-advances in formulation, characterization and applications in drug delivery; 2014. doi: 10.5772/58673.
5. Rowe RC, Sheskey PJ, Quin ME. Handbook of pharmaceutical excipients; 2009.
6. Arellano A, Santoyo S, Martin C, Ygartua P. Influence of propylene glycol and isopropyl myristate on the *in vitro* percutaneous penetration of diclofenac sodium from carbopol gels. Eur J Pharm Sci. 1999;7(2):129-35. doi: 10.1016/S0928-0987(98)00010-4, PMID 9845796.
7. Nanotechnology in Drug Delivery. In: Recent Advances in Novel Drug Carrier Systems; 2009. p. 663. doi: 10.5772/51384.
8. Shafiq-un-Nabi S, Shakeel F, Talegaonkar S, Ali J, Baboota S, Ahuja A, Khar RK, Ali M. Formulation development and optimization using nanoemulsion technique: a technical note. AAPS PharmSciTech. 2007;8(2):E12-E17. doi: 10.1208/pt0802028, PMID 17622106.
9. Maha E Elmataeeshy, M Sokar, M Bahey-El-Din, D Shaker. Enhanced transdermal permeability of terbinafine through novelnanoemulgel formulation development *in vitro* and *in vivo* characterization. Future Journal of Pharmaceutical Sciences 2018;4(1):18-28. doi: 10.1016/j.fjps.2017.07.003.
10. Syed HK, Peh KK. Identification of phases of various oil, surfactant/co-surfactants and water system by ternary phase diagram; 2014. p. 301-9. doi: 10.1109/CEC.2002.1007011.
11. Kesumawardhany B, Mita SR. Pengaruh penambahan tween 80 sebagai enhancer dalm sediaan transdermal effects of tween 80 as an enhancer in transdermal dosage form. Farmaka 2016;14(2):1-11. doi: org/10.24198/jf.v14i2.9293
12. Ansari SH, Islam F, Sameem M. Influence of nanotechnology on herbal drugs: a review. J Adv Pharm Technol Res. 2012;3(3):142-6. doi: 10.4103/2231-4040.101006, PMID 23057000.
13. Dos Santos Ramos MA, Da Silva PB, Sposito L, De Toledo LG, Bonifacio BV, Rodero CF, Dos Santos KC, Chorilli M, Bauab TM. Nanotechnology-based drug delivery systems for control of microbial biofilms: a review. Int J Nanomedicine. 2018;13:1179-213. doi: 10.2147/IJN.S146195. PMID 29520143.
14. Sari TP. Preparation and characterization of nanoemulsion encapsulating curcumin. Food Hydrocolloids. 2015;43:540-6. doi: foodhyd.2014.07.011.
15. Rai VK, Mishra N, Yadav KS, Yadav NP. Nanoemulsion as the pharmaceutical carrier for dermal and transdermal drug delivery. 2018;370:203-25. doi: 10.1016/j. jconrel.2017.11.049.
16. Shakeel F, Baboota S, Ahuja A, Ali J, Shafiq S. Skin permeation mechanism and bioavailability enhancement of celecoxib from transdermally applied nanoemulsion. J Nanobiotechnology. 2008;6:8. doi: 10.1186/1477-3155-6-8, PMID 18613981.
17. Al-shaibania AJN, Al-gburib KMH, Albo Hamraha KTK, Abd Alridhab AM. Design and characterization of candesartan cilexetil oral nanoemulsion containing garlic oil. Int J Appl Pharm. 2019;11(6):116-24. doi: 10.22159/ ijap.2019v11i6.35066.
18. Choudhury H. Recent update on nanoemulgel as topical. Drug Deliv Syst. 2017;2017:1736-51. doi: 10.1016/j.xphs.2017.03.042.
19. Ahmad M, Sahabjada, Akhtar J, Hussain A, Badaruddeen, Arshad M, Mishra A. Development of a new rutin nanoemulsion and its application on prostate carcinoma PC3 cell line. EXCLI J. 2017;16:810-23. doi: 10.17179/excli2016-668, PMID 28694767.
20. Azeem A, Rizwan M, Ahmad FJ, Iqbal Z, Khar RK, Aqil M, Talegaonkar S. Nanoemulsion components screening and selection: a technical note. AAPS PharmSciTech. 2009;10(1):69-76. doi: 10.1208/s12249-008-9178-x, PMID 19148761.
21. Chiesa M, Garg J, Kang YT, Chen G. Thermal conductivity and viscosity of water-in-oil nanoemulsions. Colloids and Surfaces A: Physicochemical and Engineering Aspects. 2008;326(1-2):67-72. doi: colsurfa.2008.05.028.
22. Rave MC, Echeverri JD, Salamanca CH. Improvement of the physical stability of oil-in-water nanoemulsions elaborated with sacha inchi oil employing ultra-high-pressure homogenization. Journal of Food Engineering. 2020;273:109801. doi: 10.1016/j.jfoodeng.2019.109801.
23. Delmas T, Piraux H, Couffin AC, Texier I, Vinet F, Poulin P, Cates ME, Bibette J. How to prepare and stabilize very small nanoemulsions. Langmuir. 2011;27(5):1683-92. doi: 10.1021/la104221q, PMID 21226496.
24. Jeong SW, Locat J, Torrance JK, Leroueil S. Thixotropic and anti-thixotropic behaviors of fine-grained soils in various flocculated systems. Engineering Geology. 2015;196:119-25. doi: . enggeo.2015.07.014.
25. Maha HL, Sinaga KR, Sinaga KR, Masfria M, Masfria M. Formulation and evaluation of miconazole nitrate nanoemulsion and cream. Asian J Pharm Clin Res. 2018;11(3):319-21. doi: 10.22159/ajpcr.2018.v11i3.22056.
26. Anwar C. Changes in yield and quality of virgin coconut oil (VCO) at various rotational speeds and length of centrifugation time; 2016. p. 51–60. doi: 10.24198.jt.vol10n2.8.
27. Helgeson ME. Colloidal behavior of nanoemulsions: interactions, structure, and rheology. Curr Opin Colloid Interface Sci. 2016;25:39-50. doi: 10.1016/j.cocis.2016.06.006.
28. Klang V, Matsko NB, Valenta C, Hofer F. Electron microscopy of nanoemulsions: an essential tool for characterisation and stability assessment. Micron. 2012;43(2-3):85-103. doi: 10.1016/j.micron.2011.07.014. PMID 21839644.
29. Sun H, Liu K, Liu W, Wang W, Guo C, Tang B, Gu J, Zhang J, Li H, Mao X, Zou Q, Zeng H. Development and characterization of a novel nanoemulsion drug-delivery system for potential application in oral delivery of protein drugs. Int J Nanomedicine. 2012;7:5529-43. doi: 10.2147/IJN.S36071. PMID 23118537.
30. Yukuyama MN. Olive oil nanoemulsion preparation using high-pressure homogenization and d-phase emulsification– A design space approach. J Drug Deliv Sci Technol. 2019;49:622-31. doi: 10.1016/j.jddst.2018.12.029. jddst.2018.12.029.

31. Klang V, Matsko N, Raupach K, El-Hagin N, Valenta C. Development of sucrose stearate-based nanoemulsions and optimisation through γ-cyclodextrin. Eur J Pharm Biopharm. 2011;79(1):58-67. doi: 10.1016/j.ejpb.2011.01.010.ejpb.2011.01.010.
32. Ghiasi Z, Esmaeli F, Khansari MG, Faramarzi MA, Amani A. Enhancing analgesic and anti-inflammatory effects of capsaicin when loaded into olive oil nanoemulsion: an in vivo study department of medical nanotechnology, school of advanced technologies in medicine, tehran university of medical sciences, Tehran. Int J Pharm. 2019. doi: 10.1016/j. ijpharm.2019.01.043.
33. Salamanca CH, Barrera Ocampo A, Lasso JC, Camacho N, Yarce CJ. Franz diffusion cell approach for pre-formulation characterization of ketoprofen semi-solid dosage forms. Pharmaceutics. 2018;10(3):1-10. doi: 10.3390/pharmaceutics 10030148, PMID 30189634.